Oscillatory Supersonic Kernel Function Method for Isolated Wings

Atlee M. Cunningham Jr.*
Convair Aerospace Division of General Dynamics, Fort Worth, Texas

The method presented uses a collocation technique with the supersonic kernel function to solve lifting surface problems on isolated wings in steady or oscillatory flow. A set of pressure functions are developed based on conical flow theory solutions which account for discontinuities in the supersonic pressure distributions. These functions permit faster solution convergence than is possible with conventional supersonic pressure functions. The method is compared with other theories and experiment for a variety of cases.

Nomenclature

a = freestream speed of sound, m/sec
a = conical coordinate
AR = aspect ratio
β = supersonic Prandtl-Glauert factor, $\beta^2 = M^2 - 1$
b_{REF} = reference length, meters—usually ½ wing chord for two-dimensional flow or ½ MAC for finite wings in three-dimensional flow
$b(\eta)$ = wing semichord at span station η, nondimensionalized by b_{REF}
C_p = pressure coefficient, $(p - p_\infty/q)$
$h(x,y)$ = mode amplitude at point x,y, non-dimensionalized by b_{REF}
i = $(-1)^{1/2}$
k = reduced frequency = $(\omega b_{REF}/U)$
m = $(\beta/\tan\Lambda_{LE})$
M = freestream Mach number = (U/a)
MAC = mean aerodynamic chord, meters
$P(\xi,\eta)$ = supersonic pressure weighting function, nondimensional
p = pressure, Newtons/meter^2
$\Delta\bar{p}(\xi,\eta)$ = lifting pressure amplitude, Newtons/meter^2
q = freestream dynamic pressure = $(\rho U^2/2)$, Newtons/meter^2
r = $[(y-\eta)^2 + (z-\zeta)^2]^{1/2}$, nondimensionalized by b_{REF}
s_0 = wing semispan, nondimensionalized by b_{REF}
U = freestream velocity, m/sec
u,v,w = velocity components in the x,y,z directions, respectively, m/sec
$w(x,y)$ = amplitude of the oscillatory downwash, m/sec
$\bar{W}(x,y)$ = $8\pi w(x,y)/U$
x,y,z = Cartesian coordinate location of the downwash point in the kernel function (x is in the direction of U), nondimensionalized by b_{REF}
x_0,y_0,z_0 = distance from an influence point to the downwash point, $(x-\xi)$, $(y-\eta)$, $(z-\zeta)$, nondimensional
ΔC_p = lifting pressure coefficient
α = angle of attack, degrees
$\Lambda_{LE},\Lambda_{TE}$ = leading and trailing edge sweep angles, degrees
ξ,η,ζ = location of an influence (or integration) point in the kernel function, nondimensionalized by b_{REF}
$\xi_m(\eta)$ = location of the midchord at span station η, nondimensionalized by b_{REF}
$\bar{\xi},\eta$ = $(\xi - \xi_m(\eta))/b(\eta)$ (η/s_0)
δ = chordwise variable of integration, nondimensional
ω = rotational frequency, rad/sec

Subscripts
LE = leading edge
MC = Mach cone (or hyperbola) boundary
TE = trailing edge
∞ = freestream conditions

Presented as Paper 73-670 at the AIAA 6th Fluid and Plasma Dynamics Conference, Palm Springs, Calif, July 16-18, 1973; submitted September 10, 1973; revision received June 12, 1974. Sponsored by NASA Langley Research Center, Contract NAS1-11565, and Convair Aerospace Division of General Dynamics Independent Research and Development Program.

Index categories: Aeroelasticity and Hydroelasticity; Structural Dynamic Analysis; Aircraft Aerodynamics (Including Component Aerodynamics).

*Project Structures Engineer, Associate Fellow AIAA.

Introduction

THE realistic prediction of steady or oscillatory aerodynamics on lifting surfaces in supersonic flow is complicated by discontinuities in the pressure distributions. These discontinuities are created by the conical regions of influence emanating from points of leading or trailing edge breaks, clipped tips, subsonic trailing edges, supersonic leading edges, deflected control surfaces, or combinations of any of these items.

The most successful methods for treating supersonic flow problems have been of the finite element type. In steady flow, the Woodward vortex panel method[1] has been developed for configurations composed of arbitrary arrays of wings and bodies. In unsteady flow, the Mach box method of Pines and Dugundji[2] or variations of the methods,[3,4] have been developed and utilized extensively for a number of years. The finite element methods have the advantage that the discontinuous supersonic influence characteristics are easily accounted for. Moreover, the assumption of pressure functions is not required to obtain a solution. For this simplicity and versatility, one pays the price in cost per solution since the finite element representation requires many elements, and hence unknown quantities, to obtain a converged solution. The Woodward method uses trapezoidal elements which yield well behaved solutions in steady flow. However, it is not applicable to unsteady flow. The Mach box methods are not so well behaved since they use a rectangular element. Swept wings must be represented with jagged leading and trailing edges which induce spacial oscillations in the pressure distributions, even in steady flow. Another disadvantage of the Mach box methods is that they use the integrated downwash technique to solve the velocity potential equation. Hence, the boundary condition of zero lift must be met in regions of influence off of the planform, i.e., the diaphragms.

Appa and Smith[5] have developed an integrated downwash technique which uses triangular elements rather than Mach boxes and hence have eliminated the jagged edges. The diaphragm is still present, although it too is simplified by treatment with triangular elements. A more recent development by Appa and Smith[6] shows promise in that they have departed from the integrated downwash method, and are investigating an integrated potential method in which the diaphragm regions are avoided.

Supersonic kernel function methods[7,8] have also been developed where assumed functions are used in a manner

similar to that employed in subsonic kernel function method. Swept planforms are easily treated as long as no Mach lines from planform discontinuities cross the surface. Also, because the acceleration potential equation is the basis, there is no need to explicitly satisfy boundary conditions off of the planform. The most serious disadvantage is that planforms with discontinuous pressure distributions are very difficult to treat. Since the assumed pressure functions are smooth, the convergence to a discontinuous distribution is very slow. Thus, the economic advantage of existing kernel function methods over finite element methods is not nearly so great (if any at all) in supersonic flow as it is in subsonic flow.

In this paper, a kernel function method is described for computing steady or oscillatory supersonic aerodynamics for isolated wings. The method differs from earlier approaches in that a special weighting function is used in the assumed pressure distributions that is derived from supersonic conical flow theory solutions.[9] Since the discontinuous characteristics are implicit in the pressure distributions, a much higher rate of solution convergence is obtained than is possible with the conventional pressure functions.

Definition of the Problem

The fundamental problem to be treated in this paper is the development of a technique to solve the integral equation that relates the normal velocity imposed by boundary conditions with the load distribution on a lifting surface in supersonic flow. The equation may be written as

$$\frac{\bar{w}(x,y)}{U} = \frac{1}{4\pi\rho U^2}\int_S \Delta\bar{p}(\xi,\eta)K(x-\xi,y-\eta,k,M)ds \quad (1)$$

The downwash $\bar{w}\ (x,y)$ is the normal velocity to the lifting surface at control point (x,y). The function $\Delta\bar{p}\ (\xi,\eta)$ is the normal lift distribution on the lifting surface at load (or integration) point (ξ,η). The kernel function K( ) is the influence function which is actually the velocity field due to an elemental normal load at point (ξ,η) on the surface. The unknown quantity is $\Delta\bar{p}\ (\xi,\eta)$ and $\bar{w}\ (x,y)$ is prescribed by the boundary conditions on the lifting surface due to surface slope and motion.

The method used to solve Eq. 1 in this paper is based on a collocation technique. The unknown pressure function is assumed to be composed of a series of polynomials weighted by a function that is characteristic of supersonic pressure distributions. The kernel function as given in the Appendix is derived from the nonplanar formulation of Harder and Rodden[10] for steady and oscillatory supersonic flow. The integration of the pressure-kernel function product is performed in essentially the same manner as done for subsonic flow[11] with exception of a change in the region of integration. The development of the necessary equations is presented in the following paragraphs.

Assumed Pressure Function

The pressure function is assumed as a series

$$\Delta\bar{p}(\xi,\eta) = qP(\xi,\eta)[g_0(\eta)f_0(\xi) + g_1(\eta)f_1(\xi) + g_2(\eta)f_2(\xi) + \ldots] \quad (2a)$$

where

$$g_n(\eta) = [a_{n0}U_0(\eta) + a_{n1}U_1(\eta) + \ldots] \quad (2b)$$

$$f_0(\xi) = U_0(\xi) = 1.0 \quad (2c)$$

$$f_n(\xi) = U_n(\xi) + U_{n-1}(\xi),\ n > 0 \quad (2d)$$

$U_n(x)$ = Tschebychev polynomial of the second kind.

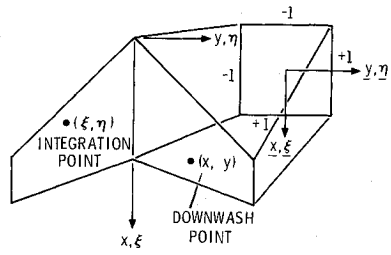

Fig. 1 Basic geometry and coordinate system.

The function $P(\xi,\eta)$ is the supersonic weighting function. The coordinates, ξ,η, are defined in the transformed plane of the surface as shown in Fig. 1.

The supersonic weighting function is based on conical flow theory solutions to the lift distributions on flat swept wings.[12] Some liberty has been taken to simplify the expressions and yet maintain the basic characteristics. At present, the function has been developed for simple trapezoidal wings; however, the extension to a general trapezoidal element is currently under development. The following derivations provide the equations necessary for wings with or without clipped tips and with subsonic or supersonic leading and trailing edges. No secondary reflections of the Mach lines are accounted for since they tend to be of second order effect and can be adequately accounted for in the collocation solution.

The basic equation for leading edge and root characteristics is the delta wing distribution. For a subsonic leading edge

$$m = \frac{\beta}{\tan\Lambda_{LE}} \leq 1.0$$

we have

$$P(\xi,\eta) = \frac{1}{\beta\left[1-\left(\frac{\bar{a}}{m}\right)^2\right]^{1/2}} \quad (3)$$

where

$$\bar{a} = \frac{\beta(\eta - y_1)}{\xi - x_1};\ x_1,y_1 = \text{Location of leading edge vertex}$$

thus

$$\frac{\bar{a}}{m} = \frac{(\eta - y_1)\tan\Lambda_{LE}}{\xi - x_1}$$

For a supersonic leading edge, $m > 1.0$

$$P(\xi,\eta) = 1 - \bar{u}(\bar{a})L(m)(1-\bar{a}^2)^{1/2} \quad (4)$$

where

$$\bar{u}(\bar{a}) = \begin{cases} 1, & \bar{a} < 1.0 \\ 0, & \bar{a} \geq 1.0 \end{cases}$$

$$L(m) = 1 - \frac{(m^2-1)^{1/2}}{4m}\left[\frac{7.0}{1.75 + \frac{1}{m}}\right]$$

The term $7.0/(1.75 + 1/m)$ which appears in the expression for $L(m)$ is the approximation used for the exact function

$$\frac{\Delta p_{ROOT}}{q} = \frac{4m\alpha}{\beta E'(m)} \approx \frac{7\alpha}{\beta\left(1.75 + \frac{1}{m}\right)}$$

where $E'\ (m)$ is the complete elliptic integral of the second kind of modulus $(1-m^2)^{1/2}$.

A tip correction is included for clipped tips. For a subsonic leading edge, $m \leq 1.0$, the lift distribution behind

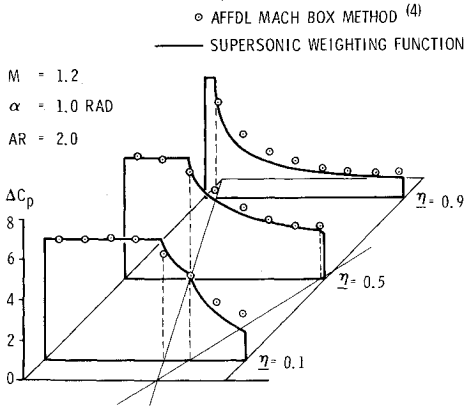

Fig. 2 Supersonic weighting function for a rectangular wing.

the tip Mach line is constant in the streamwise direction. The amplitude, a function of span only, is given as

$$P(\xi,\eta) = \frac{1}{\beta\left[1-\left(\frac{\bar{a}'}{m}\right)^2\right]^{1/2}}\left\{1-\left[\frac{(1+\bar{a}')(m+\bar{a}')}{2m(1+m)}\right]^{1/2}\right\} \tag{5}$$

where

$$\bar{a}' = \frac{\beta\eta}{x_{TIP}-(y_{TIP}-\eta)\beta} = \text{Value of "}\bar{a}\text{" along the tip Mach line at span station}$$

For a supersonic leading edge, $m > 1.0$, the lift distribution behind the tip Mach line is given as

$$P(\xi,\eta) = P(\xi,\eta)_{DELTA}\left[\frac{2}{\pi}\sin^{-1}(\bar{a}'')^{1/2}\right] \tag{6}$$

where

$P(\xi,\eta)_{DELTA}$ = Delta wing distribution given by Eq. (4)

$$\bar{a}'' = \beta\left(\frac{y_{TIP}-\eta}{x_{TIP}-\xi}\right) = \text{Value of "}\bar{a}\text{" relative to forward wing tip.}$$

The functions given above in Eqs. (5) and (6) are exact shapes as required by conical flow theory.

A final correction to the delta wing distribution is the subsonic trailing edge term. This term is approximated as a multiplicative function applied to the delta plus tip term. The function is

$$P(\xi,\eta) = P(\xi,\eta)_{DELTA+TIP}\left[\frac{2}{\pi}\sin^{-1}(\bar{a}''')^{1/2}\right] \tag{7}$$

for $0.0 \le \bar{a}''' \le 1.0$ where

$$\bar{a}''' = \frac{\xi - x_{TE}}{(x_{TEV}+\beta\eta)-x_{TE}}$$

$$x_{TE} = \eta(\tan\Lambda_{TE}) + x_{TEV} = x \text{ position of trailing edge}$$

$$x_{TEV} = x \text{ position of the trailing edge vertex}$$

thus

$$\bar{a}''' = \frac{\eta-(\xi-x_{TEV})\frac{m'}{\beta}}{\eta(1-m')}$$

$$m' = \frac{\beta}{\tan\Lambda_{TE}} < 1.0$$

The form of this approximation is not exactly correct, however, it seems to be close enough for practical purposes as experience has shown.

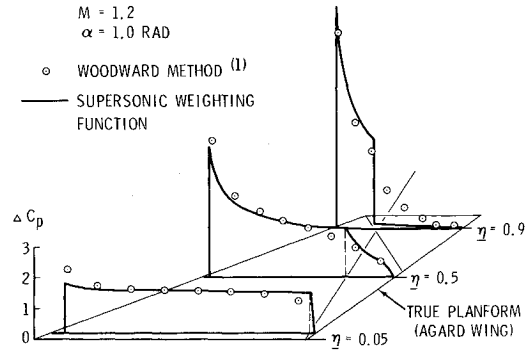

Fig. 3 Supersonic weighting function for a trapezoidal wing with subsonic leading and trailing edges.

Three examples are shown in Figs. 2–4 for the supersonic weighting function. The magnitude of the weighting function is adjusted uniformly in each case so that the shapes can be compared with other theories or experiment. The first example in Fig. 2 is for a rectangular wing, $AR = 2.0$, in steady flow at $M = 1.2$ and $\alpha = 1.0$ rad. The solid line is the weighting function simply computed at the span stations $\eta = 0.1$, 0.5, and 0.9 with the equations given in this section. The Mach lines are shown for clarity. The symbols are values computed by the AFFDL Mach box program for wing-tail configurations.[4] The second example in Fig. 3 is a swept tapered wing of the standard AGARD wing-tail configuration (the true planform is shown). The conditions are steady flow, $M = 1.2$ and $\alpha = 1.0$ rad. The solid line is again the weighting function. The symbols are results from the Woodward finite element method.[1] The disagreement at the Mach line discontinuities is due to the inability of the finite element representation to conform to such characteristics with a reasonable number of elements. The third example shown in Fig. 4 is a trapezoidal wing with a supersonic leading edge. In this case, the leading edge vertex Mach cone intersects the tip cone. Comparison with the Woodward method and experiment clearly illustrates the validity of the function.

Kernel Function

The kernel function, $K(\ )$ shown in Eq. 1 is quite complicated but can be reduced to simple form if $k = 0$ (steady flow). Under such conditions, the function is expressed as

$$K(x-\xi,y-\eta,0,M) = -\frac{2x_0}{r^2R}, \quad x_0 \ge \beta r$$
$$= 0, \quad x_0 < \beta r \tag{8}$$

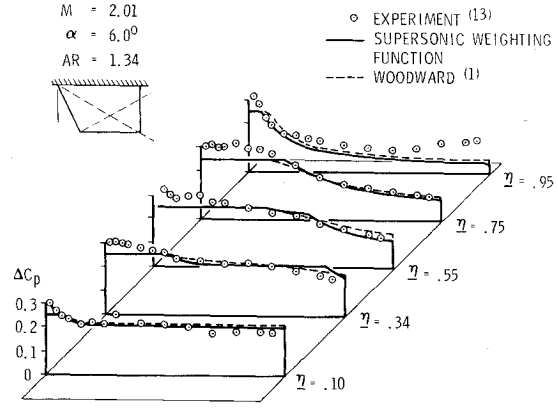

Fig. 4 Supersonic weighting function for a trapezoidal wing with supersonic leading and trailing edges.

where

$$x_0 = x - \xi$$
$$y_0 = y - \eta$$
$$r^2 = {y_0}^2$$
$$R^2 = {x_0}^2 - \beta^2 r^2$$

The characteristics of the supersonic kernel function are identical to those of the subsonic kernel for large values of x_0. For small values of x_0, particularly for $x_0 \approx \beta r$, the differences are of major importance. As can be seen in Eq. (8), the kernel has a square root singularity along the forward Mach cone emanating from the downwash point, i.e., along $x_0 = \beta r$. This singularity is useful, however, in the chordwise integration of Eq. 1 as will be shown in the next subsection.

The unsteady form of the kernel function is more complicated than that of steady flow and is given in the Appendix. The singularities are similar to those of steady flow and may be integrated in essentially the same manner as was shown in Ref. 11. The only exception, like subsonic flow, is a logarithmic singularity in the spanwise integral encountered only in unsteady flow.

Calculation of Downwash

The downwash induced by a surface on itself is unique in supersonic flow in that the downwash point is located on the boundary of the region of integration. The following discussion will present the equations for evaluating the integral. For sake of brevity, however, the development will be given only for steady flow. The unsteady equations are developed in the same manner.

Chordwise Integration

Evaluation of Eq. (1) is accomplished by first performing a coordinate transformation for the chordwise variable of integration, ξ. The integral equation is cast in the following form

$$\bar{W}(x,y) = -2 \fint_{\eta_a}^{\eta_b} \int_{-1}^{\xi_{mc}} \Delta\bar{p}(\xi,\eta) \frac{x_0}{R} \frac{b(\eta)d\xi d\eta}{s_0(y-\eta)^2} \qquad (9)$$

where

$$\bar{w}(x,y) = 8\pi\bar{w}(x,y)/U$$

Since the kernel function is singular along the forward Mach cone boundary as $(\epsilon)^{-1/2}$ for $\epsilon \to 0$, a new chordwise variable of integration, δ, will be defined as

$$\delta = \frac{1 - \xi_{mc} + z\xi}{1 + \xi_{mc}}$$

and

$$d\delta = \frac{2d\xi}{1 + \xi_{mc}}$$

Substituting δ for ξ and multiplying and dividing the integrand by $(1 - \delta^2)^{1/2}$, Eq. (1) becomes

$$\bar{w}(x,y) = -\frac{2}{s_0} \fint_{\eta_a}^{\eta_b} \left\{ \frac{(1+\xi_{mc})}{2} \int_{-1}^{1} (1-\delta^2)^{-1/2} [(1 - \delta^2)^{1/2} \Delta\bar{p}(\xi,\eta)] \frac{x_0 d\delta}{R} \right\} \cdot \frac{b(\eta)d\eta}{(y-\eta)^2}, \quad \xi_{mc} < 1 \qquad (10a)$$

and

$$\bar{w}(x,y) = -\frac{2}{s_0} \fint_{\eta_a}^{\eta_b} \left\{ \int_{-1}^{1} (1-\xi^2)^{-1/2} [(1 - \xi^2)^{1/2} \Delta\bar{p}(\xi,\eta)] \frac{x_0 d\xi}{R} \right\} \cdot \frac{b(\eta)d\eta}{(y-\eta)^2}, \quad \xi_{mc} \geq 1 \qquad (10b)$$

It should be noted that regardless of whether the Mach cone is forward ($\xi_{mc} < 1$) or aft ($\xi_{mc} > 1$) of the trailing edge, the chordwise weighting function, $(1 - \delta^2)^{-1/2}$ or $(1 - \xi^2)^{-1/2}$, is the same. As a result, the same chordwise integration scheme can be applied.

The Tschebychev-Gaussian quadrature integration formula, which is applicable to the chordwise integral in Eqs. (10), is

$$\int_{-1}^{1} (1-\xi^2)^{-1/2} f(\xi) d\xi = \frac{\pi}{J} \sum_{j=1}^{J} f(\xi_j) \qquad (11)$$

where

$$\xi_j = -\cos\left(\frac{2j-1}{2J}\pi\right)$$

and $f(\xi)$ is expressible as a polynomial of $(2J - 1)$ degree or less. Now, the chordwise integrals in Eq. 10 may be evaluated as

$$G(y,\eta) = b(\eta)(1+\xi_{mc}) \frac{\pi}{J} \sum_{j=1}^{J} (1-\delta_i^2)^{1/2} \Delta p(\xi_j,\eta) \cdot (x-\xi_j)[(x-\xi_j)^2 - \beta^2(y-\eta^2)]^{-1/2}, \quad \xi_{mc} < 1 \qquad (12a)$$

where

$$\delta_j = -\cos\left(\frac{2j-1}{2J}\pi\right), j = 1,2,\ldots J$$
$$\xi_j = \frac{1}{2}[(1+\xi_{mc})\delta_j + (\xi_{mc} - 1)]$$
$$\xi_j = [\xi_j b(\eta) + \xi_m(\eta)]$$

and as

$$G(y,\eta) = 2b(\eta) \frac{\pi}{j} \sum_{j=1}^{J} (1-\xi_j^2)^{1/2} \Delta p(\xi_j,\eta) \cdot (x-\xi_j)[(x-\xi_j)^2 - \beta^2(y-\eta)^2]^{-1/2}, \quad \xi_{mc} \geq 1 \qquad (12b)$$

where

$$\xi_j = -\cos\left(\frac{2j-1}{2J}\pi\right), \quad j = 1,2,\ldots J$$

In the existing method, no special treatment of the pressure function discontinuities has been made. The means of evaluating the integral simply depends upon the use of at least twenty or more chordwise integration points, i.e., $J \geq 20$. A scheme is under development, however, which will reduce the nominal value of J by a factor of three or four. Although the cost resulting from this practice is not significant for steady flow problems, it is very significant for unsteady flow, hence, the improvement is needed. For unsteady flow cases, in which $k \sim 1.0$ or greater, the cost reduction would be less since more integration points would be needed than for steady flow or small values of k.

Spanwise Integration

In supersonic flow, the spanwise integral is of the form

$$I(y) = \fint_{\eta_a}^{\eta_b} \frac{G(y,\eta)}{(y-\eta)^2} d\eta \qquad (13)$$

where the limits of integration, η_a and η_b, are the locations of the intersection of the Mach fore cone with the wing leading edge. Except for a weighting function, $(1 - \eta^2)^{1/2}$, and the limits η_a and η_b, Eq. (13) is identical to the equation for subsonic flow. Thus, the improper integral is evaluated with the same approach used in subsonic flow.

Let

$$G(y,\eta) = G(y,y) + (\eta - y)G'(y,y) + (\eta - y)^2 G''(y,y) + \ldots \qquad (14)$$

Adding and subtracting Eq. (14) from Eq. (13) yields

$$I(\mathbf{y}) = \int_{\eta_a}^{\eta_b} \{G(\mathbf{y},\eta) - [G(\mathbf{y},\mathbf{y}) + (\eta - \mathbf{y})G'(\mathbf{y},\mathbf{y}) + (\eta - \mathbf{y})^2 G''(\mathbf{y},\mathbf{y}) + \ldots]\} \frac{d\eta}{(\mathbf{y} - \eta)^2} + \oint_{\eta_a}^{\eta_b} [G(\mathbf{y},\mathbf{y}) + (\eta - \mathbf{y})G'(y,y) + (\eta - \mathbf{y})^2 G''(y,y) + \ldots] \frac{d\eta}{(\mathbf{y} - \eta)^2} \quad (15)$$

where the first integral may be evaluated with numerical quadrature integration techniques and the second integral evaluated analytically.

The quadrature integration is performed with a formula derived from the equations for function approximation with Tschebychev polynomials of the first kind. The approximation to a function $g(\eta')$ over the interval $(-1 \leq \eta' \leq 1)$ is

$$g(\eta') = \frac{C_0}{2} + \sum_{k=1}^{S'-1} C_k T_k(\eta') \quad (16a)$$

where

$$c_R = \frac{2}{S'} \sum_{s=1}^{S'} f(\eta_s') T_k(\eta_s') \quad (16b)$$

$$\eta_s' = -\cos\left(\frac{2s-1}{2S'}\pi\right) \quad (16c)$$

S' = Total integration chords in the range $-1 \leq \eta' \leq 1$ (16d)

If $g(\eta')$ is expressible as a polynomial degree $(S' - 1)$ or less over the interval $(-1 \leq \eta' \leq 1)$, the approximation is exact. The quadrature integration formula is derived by integrating Eq. (16a) from $\eta' = -1$ to $\eta' = +1$ and inserting Eq. (16b). The result is

$$\int_{-1}^{1} g(\eta')d\eta' = \frac{\pi}{S'} \sum_{s=1}^{S'} g(\eta_s')h(\eta_s') \quad (17)$$

where

$$h(\eta_s') = \frac{2}{\pi} \sum_{k=0}^{S'-1} T_k(\eta_s')\mathfrak{I}_k$$

and

$$\mathfrak{I}_0 = 1.0$$

$$\mathfrak{I}_k = 0, \quad k = 1,3,5,\ldots$$

$$\mathfrak{I}_k = \int_{-1}^{1} T_k'(\eta')d\eta' = \frac{-2}{(k-1)(k+1)}, \quad k = 2,4,\ldots$$

The only difference in the quadrature integration formula above and that used in the subsonic spanwise integral is the definition of $h(\eta')$.

In order to achieve a more optimum distribution of spanwise integration points, a coordinate transformation is made such that the greatest density of integration points is next to the downwash chord. This step is particularly necessary for downwash points near the leading edge. The transformation is

$$\eta_s = y_r + (\eta_s' + 1), \quad \eta_s' < -y_r \quad (18a)$$

$$\eta_s = y_r + (\eta_s' - 1), \quad \eta_s' > -y_r \quad (18b)$$

where

$$y_r = -\cos\left(\frac{nr\pi}{S'}\right), \quad r = 1,2,\ldots R, \quad n = 1,3,5,\ldots \quad (19a)$$

and

$$S = S' = n(2R + 1), \quad \text{Rectangular wings} \quad (19b)$$

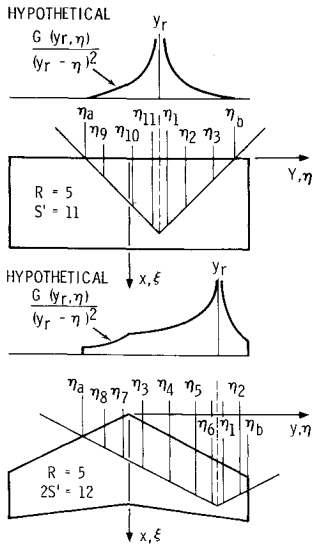

Fig. 5 Geometric relationships in the spanwise integration scheme.

$$S = 2S' = 2n(R + 1), \quad \text{Swept wings} \quad (19c)$$

The y_r defined in Eq. (19a) are the same as used in subsonic flow and are interdigitated with the η_s points by the relationship between R and S in Eqs. (19b) and (19c).

Returning to Eq. (15) the integral is evaluated as

$$I(y_r) = \frac{\pi}{S} \sum_{s=1}^{S} \frac{G(y_r,\eta_s)}{(y_r - \eta_s)^2} h(\eta_s') + Q(y_r) \quad (20a)$$

where

$$Q(y_r) = G(y_r,y_r)E_0(y_r) + G'(y_r,y_r)E_1(y_r) + G''(y_r,y_r)E_2(y_r) \quad (20b)$$

The E_n (y_r) terms are the differences between the quadrature and analytic integral evaluations

$$E_0(y_r) = \left[\frac{1}{(\eta_a - y_r)} - \frac{1}{(\eta_b - y_r)}\right] - \frac{\pi}{S} \sum_{s=1}^{S'} \frac{h(\eta_s')}{(\eta_s - y_r)^2} \quad (21a)$$

$$E_1(y_r) = \ln\left|\frac{\eta_b - y_r}{\eta_a - y_r}\right| - \frac{\pi}{S} \sum_{s=1}^{S} \frac{h(\eta_s')}{(\eta_s - y_r)} \quad (21b)$$

$$E_2(y_r) = (\eta_b - \eta_a) - \frac{\pi}{S} \sum_{s=1}^{S} h(\eta_s') \quad (21c)$$

where in the E_0 term the Mangler formula was used.[14] No terms higher than E_2 (y_r) have been found necessary, hence, the series was truncated at that point.

Shown in Fig. 5 are examples of the relationships between y_r, η_s, η_a and, η_b. Also shown are hypothetical distributions of $G(y_r, \eta_s)/(y_r - \eta)^2$ which is being integrated. The two following examples illustrate the differences between the treatment of unswept and swept trapezoidal planforms which is embodied in the definition of the spanwise functions and η:

$$\eta = \eta S_0 \quad \text{unswept leading and trailing edges} \quad (22a)$$

$$\eta = \frac{S_0}{2}(1 + \eta) \quad \text{swept trapezoidal wings (right hand wing)} \quad (22b)$$

$$\eta = -\frac{S_0}{2}(1 + \eta) \quad \text{swept trapezoidal wings (left hand wing)} \quad (22c)$$

For Eq. (22a), there are S' total integration chords on the wing and $R = (S'/n - 1)/2$ downwash chords on the right hand wing. For Eqs. (22b) and (22c), there are $2S'$ total

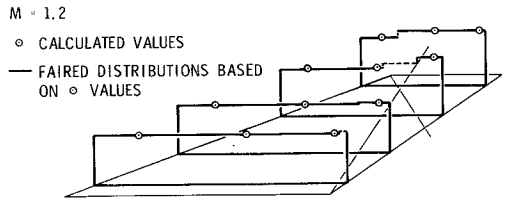

Fig. 6 Downwash induced by the supersonic weighting function in steady flow, $M = 1.2$.

integration chords and $R = (S'/n - 1)$ downwash chords on the right hand wing.

The G, G', and G'' terms are simply calculated as the coefficients of a quadratic curve fit of the chordwise integrals at $G(y_r, \eta_s)$, $G(y_r, y_r)$, and $G(y_r, \eta_1)$. The relationship between these integrals is also shown in Fig. 5. In unsteady flow, these terms will have real and imaginary parts.

Shown in Fig. 6 is an example of calculated downwash on a swept trapezoidal wing (AGARD planform) for the first term in the pressure series. This term corresponds to the supersonic weighting function shown in Fig. 3 multiplied by a constant. The case illustrated has subsonic leading and trailing edges with a clipped tip. As can be seen, the downwash distribution is quite flat and well behaved.

Solving the Boundary Value Problem

The boundary value problem is solved in the usual manner for either steady or unsteady flow by equating the calculated downwash from the pressure assumed functions to that prescribed by the boundary conditions. The vector of unknown pressure series coefficients, $\{a_{nm}\}$, in Eq. (2b) are solved for as follows

$$\{a_{nm}\} = -8\pi[A]^{-1} \left\{ \frac{\partial h(x_i,y_r)}{\partial x} + ikh(x_i,y_r) \right\}$$

where $[A]$ is the matrix of influence coefficients as derived from the evaluation of Eq. (1). The locations of the control points on the surface are prescribed as

$$x_i = -\cos\left(\frac{2i\pi}{2NC+1}\right), \quad i = 1,2,\ldots NC$$

$$y_r = \cos\left(\frac{r\pi}{2NS+1}\right), \text{ RECTANGULAR}$$

$$y_r = \cos\left(\frac{r\pi}{NS+1}\right), \text{ SWEPT} \qquad r = 1,2,\ldots(NS = R)$$

where the transformation from x_i to x_i is given below Eq. (12a). NC and NS are the number of chordwise and spanwise functions used to describe the pressure distributions. For more discussion on relationships between (NC,NS), the reader is referred to Ref. 11.

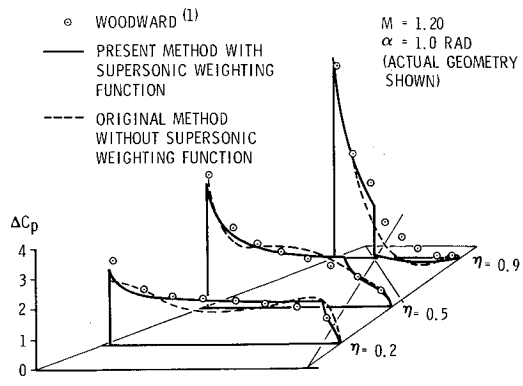

Fig. 7 Steady lift distribution on the AGARD wing.

Numerical Results

Two examples of application of the supersonic method are shown in Figs. 7 and 8. These results are preliminary in nature and are presented to show that the supersonic weighting function is valid and is superior to the functions derived from subsonic flow.

The first example in Fig. 7 is a case in which the AGARD wing is at $\alpha = 1.0$ Radian in steady $M = 1.20$ flow. The number of terms used are $NS = 4$ (spanwise) and $NC = 3$ (chordwise) on the wing. The results shown as solid curves are compared with results from the Woodward method[1] as indicated by the symbols. For comparison, the dashed curves on the wing are results computed with the original supersonic method[9] which used subsonic type chordwise and spanwise functions. It is interesting to note that the original method yields a solution which oscillates about that of the present method but it required $NC = 4$ and $NS = 6$ on the wing as compared to $NC = 3$ and $NS = 4$. More terms could be used in the original method, however, the oscillations would still persist due to the incompatibility between the assumed functions and the actual solution.

The second example in Fig. 8 is a case for a rectangular wing oscillating in a uniform translation mode at $k = 0.2$ (based on semispan) and $M = 1.20$ flow. The results of the present method (solid and dashed curves) show excellent agreement with those obtained by the AFFDL Mach Box method[4] (symbols). Both real and imaginary parts of the solution are shown. The number of terms used in the collocation solution were $NC = 3$ and $NS = 4$.

Conclusions

In this paper, a supersonic kernel function method has been presented for predicting steady and oscillatory airloads on isolated wings. The method uses a collocation technique with assumed pressure functions and the supersonic kernel function. The pressure functions differ from those used in other kernel function methods by a special weighting function. This supersonic weighting function is derived as an approximation to conical flow theory solutions for the flat plate trapezoidal wing problem. As a result, the first term in the pressure series is nearly an exact solution for uniform angle of attack which contains most of the major discontinuities that arise in supersonic flow. The downwash induced by the weighting function is shown to be very flat for such difficult configurations as a swept wing with subsonic leading and trailing edges with a clipped tip.

The method was used to obtain preliminary results for two configurations in steady and oscillatory flow. The results showed excellent agreement with existing finite element methods, which has provided momentum for refining the method into an efficient and practical computer program. The principal refinements will be involved with

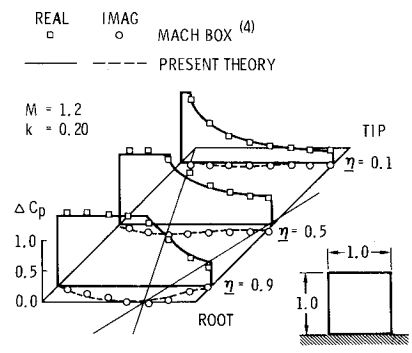

Fig. 8 Oscillatory lift on a rectangular wing for a unit translation mode.

Table 1 Kernel function series coefficients

n	a_n
1	−0.24186198
2	2.7968027
3	−24.991079
4	111.59196
5	−271.43549
6	305.75288
7	41.183630
8	−545.98537
9	644.78155
10	−328.72755
11	64.279511

improving the chordwise integration scheme such that coarser grids may be used and extending the method to include multiple leading and trailing edge breaks.

Appendix: Oscillatory Kernel Function

The oscillatory supersonic kernel function for isolated surfaces may be written as follows:

$$K(x-\xi,y-\eta,k,M) = -e^{-ikx_0}\frac{K_1}{r^2}, \quad x_0 \geq \beta r$$
$$= 0 \qquad\qquad , \quad x_0 < \beta r \quad \text{(A.1)}$$

This form is derived from the nonplanar expression given by Harder and Rodden[10] and is entirely compatible with the subsonic form. The term K_1 is

$$K_1 = K_{11} + K_{12}$$

where

$$K_{11} = \left(\frac{x_0}{R} + 1\right) e^{-ikru_1} - I_{11}$$

$$K_{12} = \left(\frac{x_0}{R} - 1\right) e^{-ikru_2} + I_{12}$$

$$\left.\begin{aligned} u_1 &= \frac{x_0 - MR}{\beta^2 r} \\ u_2 &= \frac{x_0 + MR}{\beta^2 r} \end{aligned}\right\} \qquad \beta^2 = 1 - M^2$$

For $u_1 \geq 0$,

$$I_{11} = ikre^{-ikru_1}\sum_{n=1}^{11}\frac{a_n {E_1}^n}{nc + ikr}$$

or for $u_1 < 0$

$$I_{11} = ikre^{-ikru_1}\sum_{n=1}^{11}\frac{a_n {E_1}^n}{nc - ikr} + 2\left[e^{-ikru_2} - 1 + (kr)^2\sum_{n=1}^{11}\frac{a_n}{(nc)^2 + (kr)^2}\right]$$

and

$$I_{12} = ikre^{-ikru_2}\sum_{n=1}^{11}\frac{a_n {E_2}^n}{nc + ikr}$$

where

$$\left.\begin{aligned} E_1 &= e^{-c|u_1|} \\ E_2 &= e^{-cu_2} \end{aligned}\right\} \quad c = 0.372$$

The coefficients, a_n, are given in Table I.[15]

References

[1]Woodward, F. A. and Hague, D. S., "A Computer Program for the Aerodynamic Analysis and Design of Wing-Body-Tail Combinations at Subsonic and Supersonic Speeds, Volume I: Theory and Program Utilization," ERR-FW-867, Feb. 1969, Convair Aerospace Div. of General Dynamics, Fort Worth, Texas.

[2]Pines, S., Dugundji, J., and Neuringer, J., "Aerodynamic Flutter Derivatives for a Flexible Wing with Supersonic and Subsonic Edges," *Journal of the Aerospace Sciences*, Vol. 22, No. 10, Oct. 1955, pp. 693–700.

[3]Andrew, L. V., "Unsteady Aerodynamics for Advanced Configurations, Part VI-A Supersonic Mach Box Method Applied to T-Tails, V-Tails, and Top-Mounted Vertical Tails," AFFDL-TDR-64-152, May 1969, Air Force Flight Dynamics Lab., Wright-Patterson Air Force Base, Ohio.

[4]Ii, J. M., Borland, C. J., and Hogley, J. R., "Prediction of Unsteady Aerodynamic Loadings of Non-Planar Wings and Wing-Tail Configurations in Supersonic Flow, Part 1-Theoretical Development, Program Usage and Application," AFFDL-TDR-71-108, March 1972, Air Force Flight Dynamics Lab., Wright-Patterson Air Force Base, Ohio.

[5]Appa, K. and Smith, G. C. C., "Further Developments in Consistent Unsteady Supersonic Aerodynamic Coefficients," AIAA Paper 71-177, New York, 1971.

[6]Appa, K. and Smith, G. C. C., "Finite Element Approach to the Integrated Potential Formulation of General Unsteady Supersonic Aerodynamics," Cr-112296, 1973, NASA.

[7]Cunningham, H. J., "Application of a Supersonic Kernel-Function Procedure to Flutter Analysis of Thin Lifting Surfaces," TN D-6012, Nov. 1970, NASA.

[8]Curtis, A. R. and Lingard, R. W., Jr., "Unsteady Aerodynamic Distributions for Harmonically Deforming Wings in Supersonic Flow," AIAA Paper 68-74, Jan. 1968, New York, N.Y.

[9]Cunningham, A. M., Jr., "The Application of General Aerodynamic Lifting Surface Elements to Problems in Unsteady Transonic Flow," CR-112264, Feb. 1973, NASA.

[10]Harder, R. L. and Rodden, W. P., "Kernel Function for Nonplanar Oscillating Surfaces in Supersonic Flow," *Journal of Aircraft*, Vol. 8, No. 8, Aug. 1971, pp. 677–679.

[11]Cunningham, A. M., Jr., "A Collocation Method for Predicting Oscillatory Subsonic Pressure Distributions on Interfering Parallel Lifting Surfaces," AIAA Paper 71-329, Anaheim, Calif., 1971.

[12]Cohen, Doris, "Formulas for the Supersonic Loading, Lift and Drag of Flat Swept-Back Wings with Leading Edges Behind the Mach Lines," Rept. 1050, 1951, NACA.

[13]Landrum, E. J., "A Tabulation of Wind-Tunnel Pressure Data and Section Aerodynamic Characteristics at Mach Numbers 1.61 and 2.01 for Two Trapezoidal Wings and Three Delta Wings Having Different Surface Shapes," TN D-1344, Sept. 1962, NASA.

[14]Multhopp, H., "Methods for Calculating the Lift Distribution of Wings," (Appendix I, contributed by W. Mangler), Rept. Aero-2353, Jan. 1950, Royal Aircraft Establishment, Farnborough, Hants, England.

[15]Laschka, B. and Schmid, H., "Unsteady Aerodynamic Forces on Coplanar Lifting Surfaces in Subsonic Flow (Wing-Horizontal Tail Interference)," *Jahrbuch 1967 der WGLR*, pp. 211–222.